Molecular characterization of proteolytic cleavage sites of the *Pseudomonas syringae* effector AvrRpt2

Stephen T. Chisholm*, Douglas Dahlbeck*, Nandini Krishnamurthy†, Brad Day*, Kimmen Sjolander*†, and Brian J. Staskawicz*‡

Departments of *Plant and Microbial Biology and †Bioengineering, University of California, Berkeley, CA 94720

During infection of *Arabidopsis thaliana*, the bacterium *Pseudomonas syringae* pv *tomato* delivers the effector protein AvrRpt2 into the plant cell cytosol. Within the plant cell, AvrRpt2 undergoes N-terminal processing and causes elimination of *Arabidopsis* RIN4. Previous work established that AvrRpt2 is a putative cysteine protease, and AvrRpt2 processing and RIN4 elimination require an intact predicted catalytic triad in that AvrRpt2. In this work, proteolytic events that depend on AvrRpt2 activity were characterized. The amino acid sequence surrounding the processing site of AvrRpt2 and two related sequences from RIN4 triggered AvrRpt2-dependent proteolytic cleavage of a synthetic substrate, demonstrating that these sequences are cleavage recognition sites for AvrRpt2 activity. Processing-deficient AvrRpt2 mutants were identified and shown to retain their ability to eliminate wild-type RIN4. Single amino acid substitutions were made in each of the two RIN4 cleavage sites, and mutation of both sites resulted in cleavage-resistant RIN4. Growth of *Pseudomonas* expressing AvrRpt2 was significantly higher than catalytically inactive mutants on *Arabidopsis rin4/rps2* mutant plants, suggesting there are additional protein targets of AvrRpt2 that account for the virulence activity of this effector. Bioinformatics analysis identified putative *Arabidopsis* proteins containing sequences similar to the proteolytic cleavage sites conserved in AvrRpt2 and RIN4. Several of these proteins were eliminated in an AvrRpt2-dependent manner in a transient *in planta* expression system. These results identify amino acids important for AvrRpt2 substrate recognition and cleavage as well as demonstrate AvrRpt2 protease activity eliminates multiple *Arabidopsis* proteins in a transient expression system.

bacterial virulence | cysteine protease | effector protein | plant disease resistance

Gram-negative bacterial pathogens of plants and animals use a macromolecular protein complex (the type III secretion system) to deliver proteins into the host cell cytosol (1). These proteins, referred to as effectors, collectively suppress host defenses and promote bacterial proliferation (2). Bioinformatics and biochemical studies suggest phytopathogenic bacteria secrete as many as 50 effectors into host cells (2), although the function of the majority of these is unknown. The best-characterized effectors of phytopathogenic bacteria were identified by their ability to elicit defense responses on resistant host plants. On plants unable to recognize these effectors, these proteins contribute to pathogen virulence and proliferation in the host (3, 4).

Dominant plant resistance (R) proteins confer resistance to bacteria and other pathogens expressing specific effector proteins. After effector recognition, R proteins activate intra- and intercellular signaling, resulting in localized cell death (the hypersensitive response), restricted pathogen accumulation, and systemic resistance against secondary infections (5). The majority of known R proteins from various plant species comprise a family of intracellular proteins containing a predicted nucleotide-binding domain and C-terminal leucine-rich repeats (6). Genetic data along with the presence of leucine-rich repeats in R proteins suggested direct binding of a given effector protein by its corresponding R protein. Surprisingly, physical interaction could be demonstrated for only a fraction of effector-R protein pairs, indicating an alternate mode of effector recognition may occur in many cases. Data are accumulating that support a model of indirect detection of effectors by R proteins (7). According to this model, effectors modify host proteins that are targets of their virulence activity. R proteins monitor these host targets for enzymatic modification by effectors. Upon perturbation of the monitored protein, the R protein is activated and signals for defenses (8, 9).

An instructive example of this molecular surveillance model centers on RIN4, an *Arabidopsis thaliana* protein targeted by at least three effectors from *Pseudomonas syringae*: AvrRpm1, AvrB, and AvrRpt2 (10–12). RIN4 is monitored by at least two R proteins, RPM1 and RPS2 (10–12). In the presence of AvrRpm1 or AvrB, RIN4 is phosphorylated, activating RPM1-mediated defenses (10). AvrRpt2 causes RIN4 elimination, inducing RPS2-mediated defenses (11, 12). AvrRpm1, AvrB, RPM1, and RPS2 independently coimmunoprecipitate with RIN4 (10–12). Knockdown mutants of RIN4 show constitutive activation of defense responses, implying that RIN4 may be a negative regulator of disease resistance signaling (10). Defenses are not activated in a *rin4/rps2/rpm1* triple null line, indicating that RIN4 may only negatively regulate RPS2 and RPM1 (13). These data illustrate how multiple effectors use enzymatic activities to target a single host protein and how the host uses multiple R proteins to detect these distinct modifications. In another illustration of the molecular surveillance model, the *P. syringae* effector protease AvrPphB cleaves *Arabidopsis* PBS1, activating the *Arabidopsis* R protein RPS5 (14). To date, no other effectors or R proteins that target or monitor PBS1 are known.

The effector domain of AvrRpt2 has predicted structural similarity to the cysteine protease staphopain (15). Mutation of predicted catalytic residues of AvrRpt2 abolishes its ability to eliminate RIN4 and elicit RPS2-mediated resistance (15). However, AvrRpt2 is not a constitutively functional enzyme; it requires a eukaryotic protein factor for activation (16). Recent identification of this eukaryotic factor has shown AvrRpt2 functions *in vitro* as a cysteine protease (G. Coaker and B.J.S., unpublished data).

In this work, we demonstrate proteolytic cleavage sites for AvrRpt2 occur twice in RIN4. These sites are cleaved in the presence of functional AvrRpt2 when these sequences are incorporated into a chimeric protein, confirming they are AvrRpt2 cleavage recognition motifs. Mutation of these sites in the context of full-length RIN4 generated a cleavage-resistant form of the protein. We examined processing activity of a series of AvrRpt2 cleavage site (ACS) mutants. Processing-deficient derivatives of AvrRpt2 expressed within plant cells were able to
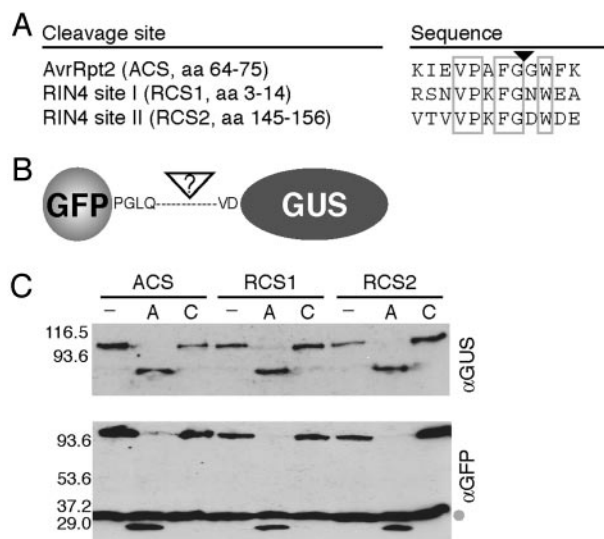
MICROBIOLOGY

Fig. 1. AvrRpt2-dependent cleavage of synthetic substrates. (*A*) Alignment of the amino acid sequence surrounding the cleavage site (filled arrowhead) of AvrRpt2 (ACS) with sequences from RIN4 (RCS1 and RCS2). Positions of these amino acids in the respective full-length proteins are given in the left column. Amino acids conserved in all sites are boxed. (*B*) Schematic representation of synthetic substrate. A translational fusion was generated between GFP and GUS such that the sequences indicated in *A* could be cloned between GFP and GUS. Single-letter codes are given for amino acids encoded by *Sal*I, *Xma*I, and *Sac*I restriction sites used for cloning purposes. (*C*) AvrRpt2-dependent cleavage of synthetic substrates. Immunoblots of protein extracts from *N. benthamiana* leaves transiently expressing synthetic substrates containing the indicated putative cleavage sites alone (lane −), with AvrRpt2:FLAG (lane A) or AvrRpt2:FLAG(C122A) (lane C). Resolved extracts were probed with αGUS (*Upper*) and αGFP (*Lower*). A crossreacting protein is indicated (shaded circle). Approximate positions of molecular mass standards are shown in kilodaltons.

eliminate RIN4, indicating that processing is not a prerequisite for AvrRpt2 protease activity. Finally, additional *Arabidopsis* proteins containing variations of the AvrRpt2 consensus cleavage sequence were identified and shown to be substrates of AvrRpt2 protease activity *in planta*. These data support the hypothesis that AvrRpt2 targets multiple *Arabidopsis* proteins during *Pseudomonas* infection.

Materials and Methods

Vectors and Strains. The sequence of all oligonucleotides and vector inserts are available by request. The sequence of all inserts was confirmed by standard methods using ABI BigDye Terminator cycle sequencing mix Ver. 3.1 (Applied Biosystems).

Synthetic Substrates. The GFP coding sequence (without a stop codon) was amplified from pGREENII-mGFP4 (17) by using the PCR with oligonucleotides that added 5′ *Bam*HI and 3′ *Sal*I restriction sites. The resulting PCR product was cloned into pCR-BLUNT II-TOPO (Invitrogen), sequenced, and transferred as a *Bam*HI–*Sal*I fragment to the binary vector pMD1 (18) to generate pMD1-GFPα7. The β-glucuronidase (GUS) sequence was amplified from pGREENII-GUS (17) by using oligonucleotides that added the following sequences to the 5′ end of the *GUS*: *Sal*I restriction site, the sequence encoding the ACS (Fig. 1*A*), or either RIN4 cleavage site (RCS1 or RCS2; Fig. 1*A*) and *Xma*I and *Xho*I sites. A *Sac*I site was added to the 3′ end of *GUS*. The resulting PCR products were cloned into pCR-BLUNT II-TOPO, sequenced, and transferred as a *Sal*I–*Sac*I fragment to pMD1-GFPα7 to generate pMD1-GFP:ACS:GUS, pMD1-GFP:RCS1:GUS, and pMD1-GFP:RCS2:GUS.

pTNT-AvrRpt2:HA and Derived Constructs. The AvrRpt2 coding sequence was amplified from pBluescript II KS-AvrRpt2 by using PCR with oligonucleotides that added restriction sites and encoded a C-terminal hemagglutinin (HA) epitope. The resulting AvrRpt2:HA PCR product was cloned into pCR-BLUNT II-TOPO and subsequently transferred to the pTNT vector (Promega) to generate pTNT-AvrRpt2:HA. AvrRpt2 processing site mutants were generated from pTNT-AvrRpt2:HA by using PCR to introduce nucleotide substitutions resulting in the indicated amino acid substitutions. For *Agrobacterium*-mediated transient expression experiments, wild-type and mutant AvrRpt2:HA constructs were transferred to pMD1.

Putative Targets. Putative target full-length cDNAs in pUNI51 (19) were obtained from the *Arabidopsis* Biological Resource Center (Columbus, OH). Individual cDNAs were amplified by using oligonucleotides that added a 5′ *Xho*I site and a 3′ HA epitope; TGA stop codon; and *Sac*I, *Kpn*I, and *Sal*I sites. Resulting PCR products were cloned into pCR-BLUNT II-TOPO. HA-tagged cDNAs were transferred as *Xho*I/*Sac*I fragments to pMD1-T7, which encodes a 5′ T7 epitope in frame with the cDNAs.

In Vitro Transcription and Translation. The TnT Quick-Coupled transcription/translation system (Promega) was used following the manufacturer's instructions. Briefly, ACS mutants were transcribed and translated in rabbit reticulocyte lysates in the presence of [^{35}S]methionine (Amersham Pharmacia). Protein samples were collected at 20-min intervals, separated by denaturing PAGE, and exposed to a phosphorimaging screen to detect radiolabeled AvrRpt2:HA.

Plant Growth, Bacterial Inoculations, and Growth Assays. Inoculations of *Arabidopsis* were performed on 5- to 6-week-old plants grown at 22°C under 8-h light and 16-h dark per day. *P. syringae* pv. *tomato* DC3000 strains were grown for 40–48 h at 28°C on *Pseudomonas* agar F (MP Biomedicals, Aurora, OH) containing 100 μg·ml^{-1} rifampicin and 25 μg·ml^{-1} kanamycin. Cells were harvested and suspended at 5×10^4 colony-forming units·ml^{-1} in 10 mM MgCl$_2$ and injected into the intercellular leaf space by using a needleless syringe. To quantify bacterial growth at 4 days postinoculation, two 20-mm^2 plant tissue samples were taken from inoculated zones, pooled, and ground in 10 mM MgCl$_2$; appropriate sample dilutions were then plated on NYG agar (20) containing 50 μg·ml^{-1} rifampicin and 12.5 μg·ml^{-1} kanamycin and cyclohexamide. Three replicates were taken for each sample.

Nicotiana benthamiana plants were grown for 4–6 weeks at 24°C under 8-h light and 16-h dark per day. All pMD1 constructs were introduced into *Agrobacterium tumefaciens* C58C1 by using triparental mating (21). Growth and harvesting of *A. tumefaciens* cells and plant infiltrations were performed as described (15). For single infiltrations, *Agrobacterium* suspensions were diluted to OD$_{600}$ of 0.3 with infiltration medium; for coinfiltrations, equal volumes of *Agrobacterium* strains were mixed so that each strain was infiltrated at an OD$_{600}$ of 0.3.

Immunoblots. Total protein extracts were collected from *N. benthamiana* leaves by using standard procedures. Briefly, tissue within infiltrated zones was collected by using two no. 7 cork borers (1.4-cm diameter), ground in 150 μl of 2× Laemmli buffer [10% (vol/vol) 2-mercaptoethanol/6% (wt/vol) SDS/20% (vol/vol) glycerol/0.2 mg/ml bromophenol blue] and boiled for 5 min. Equal volumes of protein extract were separated by using denaturing PAGE, and immunoblotting was performed according to standard procedures (22) with the following antibodies: mouse monoclonal anti-HA (1:1,000 dilution, Covance, Berkeley, CA), mouse monoclonal anti-T7 (1:1,000; Novagen), mouse monoclonal anti-FLAG (1:1,000; Sigma), mouse monoclonal

anti-GFP (1:1,000; Covance), rabbit polyclonal anti-GUS (1:1,000; Molecular Probes), and rabbit polyclonal anti-RIN4 (1:10,000; gift of J. Dangl, University of North Carolina, Chapel Hill, NC). Secondary goat anti-mouse IgG–horseradish peroxidase conjugate (1:5,000; Bio-Rad) or goat anti-rabbit IgG–horseradish peroxidase conjugate (1:5,000; Bio-Rad) was used as appropriate to detect primary antibodies. Signals were visualized by chemiluminescence by using Supersignal West Pico reagents (Pierce).

Identification of *Arabidopsis* Proteins with Putative Cleavage Sites. Global homologs (proteins aligning over their entire lengths) to RIN4 were gathered from the National Center for Biotechnology Information nonredundant database by using FLOWER-POWER, a hidden Markov model (HMM)-based iterative search method (http://phylogenomics.berkeley.edu/flowerpower). The conserved region of RIN4 and homologs was identified, and an HMM was constructed to represent the region encompassing the cleavage site. The HMM was used to score *Arabidopsis* and rice databases, and sequences with significant per-person reverse scores were retrieved and aligned to the HMM. A second HMM was created from this alignment, and the *Arabidopsis* database (TIGR, release version 5) was searched to identify remotely related sequences. A combination of HMM scores and alignment editing was used to identify a set of 111 sequences as putative substrates of AvrRpt2. To increase the precision of our prediction, a conservative subset of 19 sequences was identified containing a conserved PxFGxW motif. All HMMs used in our experiments were constructed by using the University of California Santa Cruz HMM software suite (www.cse.ucsc.edu/research/compbio/sam.html). The HMMs constructed for RIN4 and the cleavage site in these analyses can be accessed from the Berkeley Phylogenomics Group HMM library web site (http://phylogenomics.berkeley.edu/phylofacts). Alignment editing was performed by using BELVU (www.cgb.ki.se/cgb/groups/sonnhammer/Belvu.html).

Results

Sequences in RIN4 Similar to the AvrRpt2 Processing Site Are Cleaved in the Presence of AvrRpt2. After type III secretion system-mediated delivery to the plant cell, the *P. syringae* effector AvrRpt2 is processed between G71 and G72 (23). This cleavage requires an intact predicted catalytic triad in AvrRpt2, suggesting it is a self-processing event (15). Comparison of AvrRpt2 and RIN4 using MEME (Multiple Expectation maximization for Motif Elicitation) (24) identified two RIN4 sequences (Fig. 1A, RCS1 and RCS2) similar to the AvrRpt2 processing site (Fig. 1A, ACS). During the course of this work, Jones and Takemoto (25) also identified these RIN4 sequences and suggested they function as cleavage sites for AvrRpt2 protease activity. To determine whether these sequences trigger AvrRpt2-dependent cleavage, we constructed a synthetic substrate for AvrRpt2 protease activity.

The indicated 12-aa sequences from AvrRpt2 and RIN4 (Fig. 1A) were included in a translational fusion between GFP and GUS (Fig. 1B). Sequences encoding ACS, RCS1, and RCS2 were inserted between the GFP and GUS coding regions to generate GFP-ACS-GUS, GFP-RCS1-GUS, and GFP-RCS2-GUS. It was anticipated that if ACS, RCS1, and RCS2 contained cleavage sites, these substrates would be cleaved in the presence of AvrRpt2, separating the GFP and GUS portions of the fusion. Using *A. tumefaciens*-mediated transient expression in *N. benthamiana* leaves, these synthetic substrates were coexpressed with AvrRpt2:FLAG or the proteolytically deficient AvrRpt2:FLAG(C122A) mutant, in which alanine is substituted for the predicted catalytic cysteine (15). As seen in Fig. 1C, full-length GFP-ACS-GUS, GFP-RCS1-GUS, and GFP-RCS2-GUS accumulated when expressed alone or when coexpressed
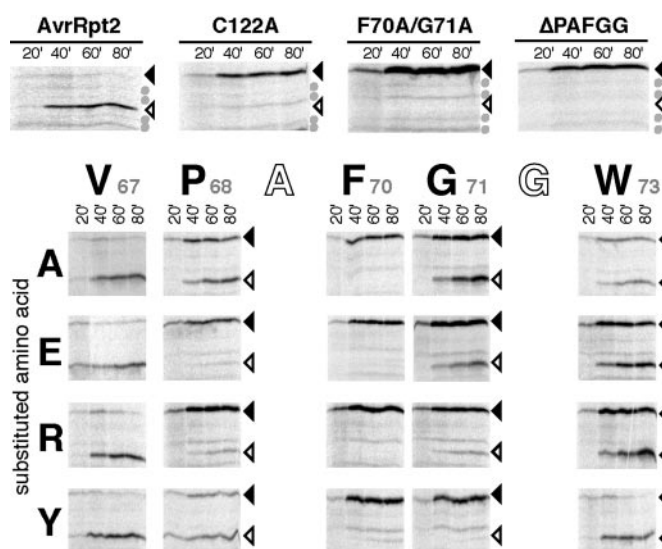

Fig. 2. Processing of AvrRpt2:HA mutants in rabbit reticulocyte lysates. The indicated forms of AvrRpt2:HA were expressed from a T7 promoter in rabbit reticulocyte lysates in the presence of [^{35}S]methionine. After the addition of template DNA, protein samples were collected at the indicated time points and resolved by using denaturing PAGE. A phosphorimaging screen was used to detect radiolabeled proteins. (*Upper*) Control reactions. (*Lower*) Conserved residues (numbered, filled amino acids) of the AvrRpt2:HA cleavage site were substituted with the indicated amino acids and analyzed as above. Filled arrowheads, unprocessed AvrRpt2:HA; open arrowheads, processed AvrRpt2:HA; filled circles, background protein bands.

with AvrRpt2:FLAG(C122A). However, when these synthetic substrates were coexpressed with functional AvrRpt2:FLAG, the GFP and GUS cleavage products accumulated (Fig. 1C), indicating AvrRpt2 cleaves the ACS, RCS1, and RCS2 sequences. This result suggests the amino acid residues common to ACS, RCS1, and RCS2 (boxed in Fig. 1A) are variations of a consensus cleavage sequence (VPxFGxW, where x indicates any amino acid) for AvrRpt2 protease activity.

In Vitro and in Planta Analyses of AvrRpt2 Processing Site Mutants. We predicted ACS mutants with substitutions that alter recognition and cleavage by AvrRpt2 would undergo processing at reduced rates. In an *in vitro* transcription and translation system, AvrRpt2:HA accumulated primarily as the processed form at the 40-, 60-, and 80-min time points (Fig. 2). Proteolytically deficient AvrRpt2:HA(C122A) accumulated as unprocessed protein at all time points (Fig. 2). The AvrRpt2:HA(F70A/G71A) double mutant accumulated as the unprocessed form (Fig. 2). AvrRpt2:HA(ΔPAFGG), a cleavage site deletion mutant that lacks five amino acids including G71 and G72, also accumulated as unprocessed protein (Fig. 2). In all cases, several faint protein bands that do not correspond to unprocessed or processed AvrRpt2 were detected (Fig. 2 *Upper*, gray circles); the nature of these bands was not determined.

To clarify the relative contribution of the five conserved amino acids (VPxFGxW) within the ACS to AvrRpt2:HA processing, each position was substituted with representative small, acidic, basic, and aromatic amino acids (alanine, glutamic acid, arginine, and tyrosine, respectively), and processing efficiency of these mutants was monitored. Although the majority of mutants were expressed at levels similar to AvrRpt2:HA, these substitutions had a wide range of effects on processing (Fig. 2). Some ACS mutants, such as AvrRpt2:HA(V67A) and (W73Y), processed at rates near wild type. Mutants such as (P68A) and (W73A) accumulated as approximately equal amounts of processed and unprocessed protein. Only mutations of F70, specif-
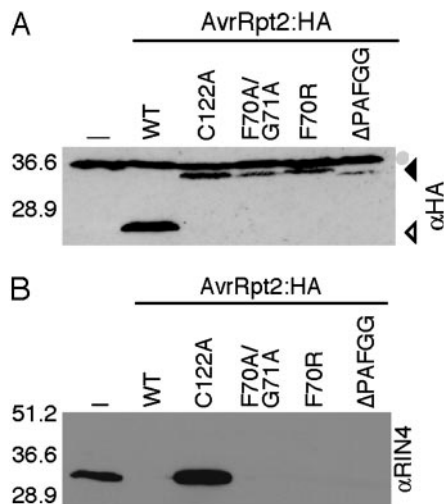
Fig. 3. Processing-deficient AvrRpt2:HA mutants prevent T7:RIN4 accumulation *in planta*. The indicated forms of AvrRpt2:HA (−, no AvrRpt2:HA) were coexpressed with T7:RIN4 in *N. benthamiana* leaves. Protein extracts were resolved by denaturing PAGE and used for immunoblot analyses. Approximate positions of molecular mass standards are shown. (*A*) Processing of AvrRpt2:HA forms *in planta*. AvrRpt2:HA (WT) accumulates as processed protein (open arrowhead). Catalytically deficient AvrRpt2:HA(C122A) and ACS mutants AvrRpt2:HA(F70A/G71A), (F70R), and (ΔPAFGG) accumulate as unprocessed proteins (filled arrowhead). Filled circle, crossreacting protein. (*B*) T7:RIN4 does not accumulate in the presence of processing-deficient AvrRpt2:HA. RIN4 antisera detects T7:RIN4 expressed alone (−) or with AvrRpt2:HA(C122A). T7:RIN4 is not detected when coexpressed with AvrRpt2:HA or AvrRpt2:HA(F70A/G71A), (F70R), or (ΔPAFGG).

Fig. 4. T7:RIN4 is cleaved at two sites *in planta*. (*A*) T7:RIN4 or the indicated T7:RIN4 mutants were coexpressed in *N. benthamiana* leaves with RPS2:HA and GFP (lane g), AvrRpt2:FLAG (lane A), or AvrRpt2:FLAG(C122A) (lane C). X, noninfiltrated leaf. Protein extracts were resolved by denaturing PAGE and used for immunoblot analyses with αRIN4. Approximate positions of molecular mass standards are shown. (*B*) RIN4 amino acid sequence. Boxed regions, conserved portions of AvrRpt2 cleavage recognition sequences; underlined regions, additional occurrences of FG sequence.

ically (F70A) and (F70R), seemed to abolish processing. Because the majority of the ACS mutants functioned as substrates for AvrRpt2-dependent protease cleavage, AvrRpt2 may cleave many variations of the sequence VPxFGxW.

To determine the processing-deficient mutants' ability to eliminate RIN4, AvrRpt2:HA(F70A/G71A), (F70R), and (ΔPAFGG) were transferred to the binary vector pMD1. Wild-type and mutant AvrRpt2:HA variants were coexpressed with an epitope-tagged form of RIN4 (T7:RIN4) in *N. benthamiana* leaves by using *Agrobacterium*-mediated transient expression. Immunoblot analysis shows that transiently expressed AvrRpt2:HA accumulates as the processed form (Fig. 3*A*). The AvrRpt2:HA(C122A), (F70A/G71A), (F70R), and (ΔPAFGG) mutants accumulate as unprocessed protein (Fig. 3*A*). When AvrRpt2:HA and T7:RIN4 were coexpressed *in planta*, T7:RIN4 did not accumulate (Fig. 3*B*). However, T7:RIN4 accumulated in the presence of the catalytically deficient AvrRpt2:HA(C122A) (Fig. 3*B*). Coexpression of processing-deficient AvrRpt2:HA prevented accumulation of T7:RIN4 (Fig. 3*B*), indicating these mutants still mediate T7:RIN4 elimination. This result suggests that although an intact catalytic triad is necessary for AvrRpt2 elimination of RIN4, processing is not strictly required.

RIN4 Is Cleaved at Two Sites *in Planta*. Transcription and translation of ACS mutants confirmed that mutation of the phenylalanine in the ACS is sufficient to prevent AvrRpt2 processing (Figs. 2 and 3*A* and ref. 16). RIN4 contains two cleavage motifs (RCS1 and RCS2, Fig. 1*A*) sufficient to elicit AvrRpt2-mediated substrate cleavage (Fig. 1*C*). It remained unclear whether these sites are cleaved in the context of full-length RIN4 protein. After AvrRpt2-mediated cleavage, RIN4 is rapidly eliminated, making recovery and direct sequencing of *in vivo* cleavage products impractical. Therefore, to determine whether AvrRpt2 cleaves T7:RIN4 at RCS1, RCS2, or
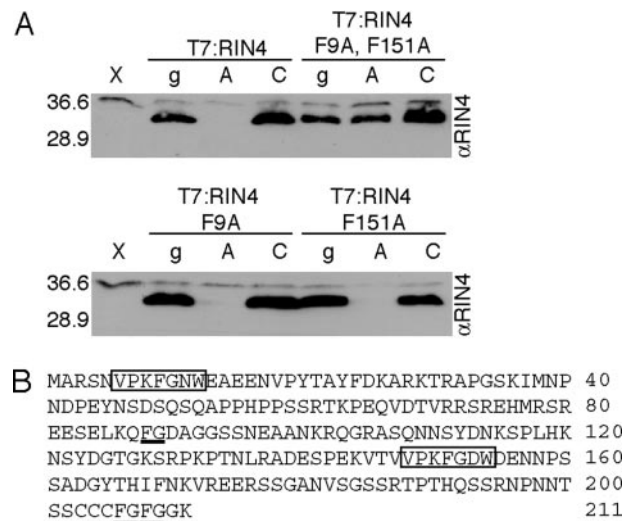
both, mutants of T7:RIN4 were generated in which the conserved phenylalanine was mutated to alanine in RCS1 (F9A), RCS2 (F151A), or both sites. T7:RIN4 mutants were transiently coexpressed with AvrRpt2:FLAG in *N. benthamiana* leaves, and T7:RIN4 elimination was monitored by immunoblot. As with wild-type protein, T7:RIN4(F9A) and T7:RIN4(F151A) were not detected when coexpressed with AvrRpt2:FLAG but accumulated when expressed alone or with AvrRpt2:FLAG(C122A) (Fig. 4*A*). The T7:RIN4(F9A/F151A) mutant accumulated when coexpressed with AvrRpt2:FLAG (Fig. 4*A*), indicating this double mutant is resistant to AvrRpt2 protease activity. This finding demonstrates that AvrRpt2:FLAG cleaves RIN4 at both RCS1 and RCS2 and that cleavage at either site is sufficient to trigger RIN4 elimination in the transient expression system. RIN4 contains three other occurrences of an FG amino acid sequence (Fig. 4*B*, underlined). Because AvrRpt2 apparently does not cleave these sequences, additional amino acids of the VPxFGxW consensus cleavage sequence must be required for substrate recognition.

AvrRpt2 Protease Activity Eliminates *Arabidopsis* Proteins in Addition to RIN4. AvrRpt2 contributes to pathogen virulence in *Arabidopsis* plants lacking the R protein RPS2, as *P. syringae* pv *tomato* strain DC3000 (*Pst*) expressing AvrRpt2 accumulates to a higher level *in planta* than *Pst* lacking AvrRpt2 (3). If elimination of RIN4 were the only virulence function of AvrRpt2, on plants lacking RIN4, *Pst* expressing AvrRpt2 would grow no better than those lacking the effector. Because RIN4 depletion activates RPS2-mediated resistance responses that include host cell death, plants deficient in RIN4 can only be recovered in an *Arabidopsis* rps2 background. Thus, to determine the effect of AvrRpt2 on *Pseudomonas* growth in plants lacking RIN4, we infected rin4/rps2 plants with bacteria expressing GFP, AvrRpt2, and the catalytically deficient mutants AvrRpt2(C122A) and (H208A) (Fig. 5*A*). At 4 days postinoculation, growth of *Pst* (*avrRpt2*) was restricted on Col-0 plants relative to *Pst*(*GFP*), *Pst*(*C122A*), and *Pst*(*H208A*). All strains accumulated to a similar level on rps2 plants. On rin4/rps2 *Arabidopsis*, *Pst*(*avrRpt2*) accumulated to
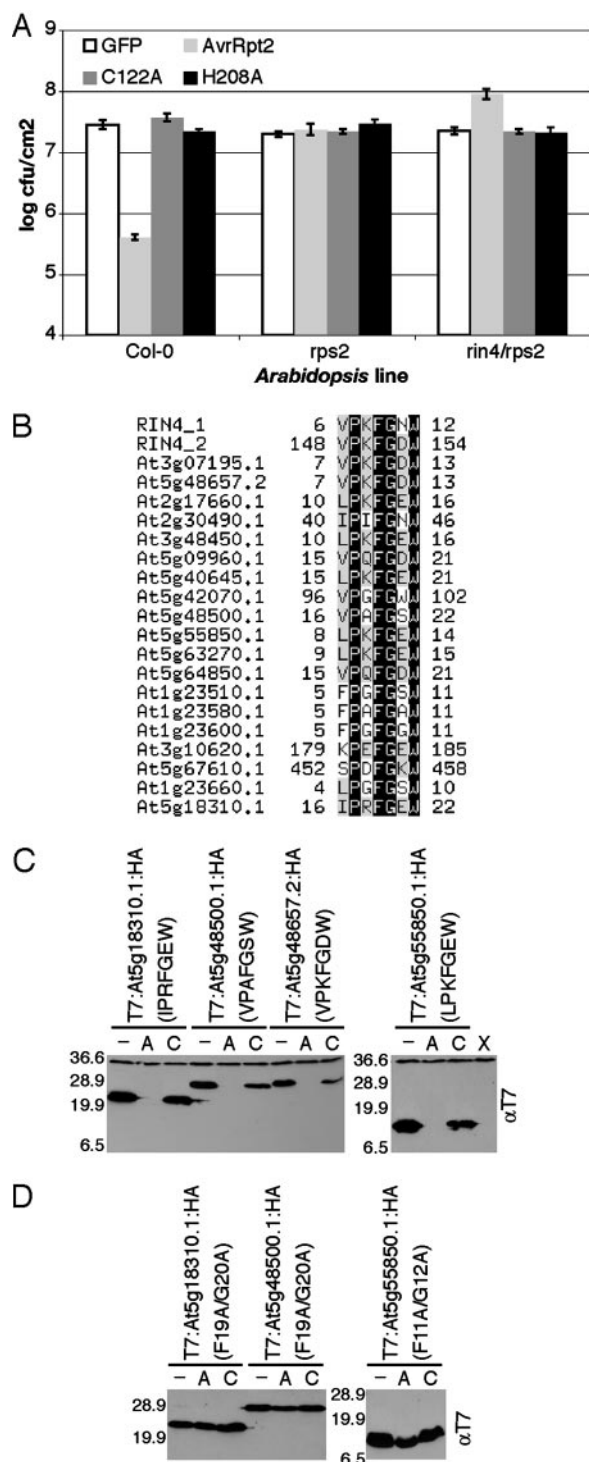
A

(graph: log cfu/cm2 vs *Arabidopsis* line)

Legend: □ GFP, AvrRpt2, C122A, ■ H208A

Lines: Col-0, rps2, rin4/rps2

B

locus	start	sequence	end
RIN4_1	6	VPKFGNW	12
RIN4_2	148	VPKFGDW	154
At3g07195.1	7	VPKFGDW	13
At5g48657.2	7	VPKFGDW	13
At2g17660.1	10	LPKFGEW	16
At2g30490.1	40	IPIFGNW	46
At3g48450.1	10	LPKFGEW	16
At5g09960.1	15	VPQFGDW	21
At5g40645.1	15	VPKFGEW	21
At5g42070.1	96	VPGFGWW	102
At5g48500.1	16	VPAFGSW	22
At5g55850.1	8	LPKFGEW	14
At5g63270.1	9	LPKFGEW	15
At5g64850.1	15	VPQFGDW	21
At1g23510.1	5	FPGFGCW	11
At1g23580.1	5	FPAFGAW	11
At1g23600.1	5	FPGFGCW	11
At3g10620.1	179	KPEFGEW	185
At5g67610.1	452	SPDFGKW	458
At1g23660.1	4	LPGFGSW	10
At5g18310.1	16	IPRFGEW	22

C

(immunoblot panels)
T7:At5g18310.1:HA (IPRFGEW), T7:At5g48500.1:HA (VPAFGSW), T7:At5g48657.2:HA (VPKFGDW), T7:At5g55850.1:HA (LPKFGEW); lanes −, A, C, X; αT7; markers 36.6, 28.9, 19.9, 6.5

D

(immunoblot panels)
T7:At5g18310.1:HA (F19A/G20A), T7:At5g48500.1:HA (F19A/G20A), T7:At5g55850.1:HA (F11A/G12A); lanes −, A, C; αT7; markers 28.9, 19.9, 6.5

Fig. 5. AvrRpt2-dependent cleavage of *Arabidopsis* proteins. (*A*) AvrRpt2 contributes to bacterial virulence on *Arabidopsis rin4/rps2* plants. *P. syringae* pv *tomato* strain DC3000 (*Pst*) expressing GFP, AvrRpt2, or catalytically deficient AvrRpt2 C122A or H208A were inoculated into *Arabidopsis* Col-0 and the indicated Col-0 mutant lines. Bacterial growth was quantified at 4 days postinoculation. (*B*) Alignment of putative ACS in *Arabidopsis* proteins. The *Arabidopsis* locus identifier is shown, followed by the start index, the sequence, and the end index of the site. RCS1 and RCS2 are represented as RIN4_1 and RIN4_2. Completely conserved residues are black, and similar residues are gray. (*C*) Putative targets do not accumulate in the presence of AvrRpt2. The indicated epitope-tagged proteins were expressed in *N. benthamiana* leaves alone (−), with AvrRpt2:FLAG (lane A), or with AvrRpt2:FLAG(C122A) (lane C). X, noninfiltrated leaf. Putative cleavage site

higher levels than *Pst*(*GFP*), *Pst*(*C122A*), or *Pst*(*H208A*). A simple interpretation of these data is that AvrRpt2 has additional virulence targets in *Arabidopsis* and that an intact catalytic triad is necessary for AvrRpt2 virulence activity.

We hypothesized that proteins containing variations of the consensus cleavage sequence VPxFGxW are targets of AvrRpt2 protease activity and, therefore, possible targets of its virulence activity. We searched the *Arabidopsis* genome for sequences encoding known or predicted proteins containing variations of this site. The search was optimized to facilitate detection of remotely related sequences (Table 1, which is published as supporting information on the PNAS web site); however, this method increased the likelihood of including false positives. To aid experimental validation, we identified a high-confidence subset of 19 sequences (Fig. 5*B*) that had a conserved PxFGxW motif and shared similarity to the region flanking RCS1 and RCS2. To determine whether these proteins are substrates of AvrRpt2, we obtained full-length cDNA clones (19) for genes encoding several of the putative targets. Full-length cDNAs were transferred to a binary vector such that T7 and HA epitope tags were added to the 5′ and 3′ ends of the gene, respectively. These constructs were then transiently coexpressed in *N. benthamiana* with AvrRpt2:FLAG forms. Putative targets accumulated when expressed alone or in the presence of AvrRpt2:FLAG(C122A) (Fig. 5*C*). When these proteins were coexpressed with AvrRpt2:FLAG, neither the T7 or HA epitope of these proteins was detected (Fig. 5*C* and data not shown). Elimination of these proteins in the presence of functional AvrRpt2 indicates they are targets of AvrRpt2 protease activity.

To verify that the putative cleavage sites in T7:At5g18310.1:HA, T7:At5g48500.1:HA, and T7:At5g55850.1:HA were the sequences targeted by AvrRpt2 protease activity, cleavage-resistant forms of these sites were generated. The conserved phenylalanine and glycine residues were simultaneously substituted with alanine residues. These proteins were transiently expressed in *N. benthamiana* leaves. As shown in Fig. 5*D*, these cleavage site mutants accumulate when expressed alone and when coexpressed with AvrRpt2:FLAG or AvrRpt2:FLAG(C122A), indicating that they are resistant to proteolytic cleavage. This finding confirms that AvrRpt2-mediated elimination of these proteins requires the sequence used to identify them as putative AvrRpt2 virulence targets.

Discussion

Modification of host proteins by pathogen effectors modulates host pathways to suppress defenses and favor pathogen proliferation. In the case of plant pathogenic bacteria such as *P. syringae*, it seems plants evolved R proteins capable of detecting distinct modifications of host proteins targeted by one or more effectors. To better understand how effectors target host proteins, we characterized protease activity of the *P. syringae* effector AvrRpt2 and identified potential host targets of this protease.

During infection of *Arabidopsis*, the *P. syringae* pv. *phaseolicola* effector protease AvrPphB is autoproteolytically processed and cleaves a host protein, PBS1 (14). Peptide sequencing of processed AvrPphB and cleaved PBS1 revealed that in both cases cleavage occurs C-terminal to a 3-aa motif, GDK (14). A conserved cleavage recognition sequence was identified in common between AvrRpt2 and RIN4, an *Arabidopsis* protein eliminated in an AvrRpt2-dependent manner. There are two variations of this sequence in RIN4 (Fig. 1*A*, RCS1 and RCS2). Analyses of RIN4 mutants in which these sites were mutated indicate AvrRpt2 cleaves both

amino acid sequences are given in parentheses. Protein extracts were resolved by denaturing PAGE and used for immunoblot analyses with αT7. Approximate positions of molecular mass standards are shown. (*D*) Mutation of putative cleavage sites prevents AvrRpt2-dependent protein elimination. The indicated epitope-tagged proteins were expressed in *N. benthamiana* and analyzed as in *C*. Amino acid mutations for each protein are listed in parentheses.

RCS1 and RCS2. Furthermore, cleavage-resistant RIN4 was generated by simultaneously mutating both RCS1 and RCS2. These experiments were performed by using an *in planta* transient expression system; it will be interesting to determine the phenotype of *Arabidopsis* plants expressing cleavage-resistant RIN4. Will these plants be able to detect AvrRpt2 activity and activate defense responses? Will AvrRpt2 activity still interfere with RPM1-mediated resistance to AvrB and AvrRpm1, two other effectors that modify RIN4? Will cleavage-resistant RIN4 still be phosphorylated in the presence of AvrB or AvrRpm1, thereby activating RPM1-mediated resistance?

In addition to determining that RCS1 and RCS2 are cleaved by AvrRpt2 in T7:RIN4, we observed AvrRpt2-dependent cleavage of synthetic substrates containing these sequences (Fig. 1*C*) or the ACS (Fig. 1*A*). These results suggest AvrRpt2 substrate cleavage requires only the 7-aa consensus sequence VPxFGxW. A majority of AvrRpt2 mutants in which this sequence was altered retained their ability to be processed, indicating AvrRpt2 potentially cleaves a variety of amino acid sequences. Interestingly, processing-deficient forms of AvrRpt2 were able to eliminate RIN4 *in planta*, indicating AvrRpt2 amino acids 1–71 do not inhibit its protease activity in the transient expression system. As with all effectors delivered to the host cell via the type III secretion system, the N terminus of AvrRpt2 includes type III secretion signals. Within the plant cell, AvrRpt2 is associated with the plasma membrane. Processing of AvrRpt2 may remove type III secretion signals and allow membrane localization. Indeed, Jin *et al.* (16) observed accumulation of a proteolytically inactive (therefore unprocessed) version of an AvrRpt2-GFP fusion in chloroplasts of protoplasts, suggesting unprocessed AvrRpt2 may be targeted to the chloroplast. However, the roles of the AvrRpt2 N terminus or its processing in proper localization have yet to be firmly established.

AvrRpt2 contributed to *Pseudomonas* virulence in *Arabidopsis* rin4/rps2 plants; however, it did not have a virulence function in rps2 plants (Fig. 5*A*). Belkhadir *et al.* (13) observed similar results using a weakly virulent *Pseudomonas* strain but saw a modest AvrRpt2 virulence function in rps2 plants and concluded RIN4 negatively regulates AvrRpt2 virulence function. These data, as well as the work of Lim and Kunkel (26), support the hypothesis that AvrRpt2 targets multiple *Arabidopsis* proteins.

The *Pseudomonas* effectors AvrB and AvrRpm1 also target proteins in addition to RIN4 (13). The activities of other effector proteases, specifically *Xanthomonas campestris* XopD and AvrXv4 that remove SUMO modifications from proteins, clearly target more than one host protein, although the identities of these host targets are not yet known (27, 28). This finding suggests targeting of multiple host proteins may be a common strategy used by a number of effectors. Having determined AvrRpt2, substrate recognition requires <12 substrate amino acids, and AvrRpt2 recognizes many alterations of a 7-aa consensus recognition sequence, we identified *Arabidopsis* proteins that contain variations of this sequence. Four such proteins were eliminated *in planta* in an AvrRpt2-dependent manner. Mutation of two conserved residues in their respective cleavage sites generated cleavage-resistant forms of three of these proteins. These results indicate genomic data can be used to accurately predict targets of AvrRpt2. These findings are in contrast to work with the *Pseudomonas* effector protease AvrPphB (14). Shao *et al.* (14) identified two *Arabidopsis* kinases related to the AvrPphB substrate PBS1, including one that contained the GDK motif and all other amino acids required for cleavage of PBS1, and tested them for cleavage by AvrPphB. Neither protein was cleaved by AvrPphB, suggesting the GDK sequence is not sufficient to trigger cleavage.

AvrRpt2 cleaves itself at VPAFGGW and eliminates *Arabidopsis* proteins containing the sequences VPKFGNW, VPKFGDW, VPAFGSW, IPRFGEW, and LPKFGEW. It is reasonable to assume AvrRpt2 cleaves other variations of the (V/I/L)PxFGxW sequence. Thus, AvrRpt2 may eliminate a large number of host proteins during *Pseudomonas* infection. The elimination of these proteins in *Arabidopsis* needs to be confirmed, and the roles of these various proteins in susceptibility and resistance need to be established.

1. Galan, J. E. & Collmer, A. (1999) *Science* **284,** 1322–1328.
2. Alfano, J. R. & Collmer, A. (2004) *Annu. Rev. Phytopathol.* **42,** 385–414.
3. Chen, Z., Kloek, A. P., Boch, J., Katagiri, F. & Kunkel, B. N. (2000) *Mol. Plant–Microbe Interact.* **13,** 1312–1321.
4. Abramovitch, R. B. & Martin, G. B. (2004) *Curr. Opin. Plant Biol.* **7,** 356–364.
5. Nimchuk, Z., Eulgem, T., Holt, B. F., III, & Dangl, J. L. (2003) *Annu. Rev. Genet.* **37,** 579–609.
6. Belkhadir, Y., Subramaniam, R. & Dangl, J. L. (2004) *Curr. Opin. Plant Biol.* **7,** 391–399.
7. Van der Biezen, E. A. & Jones, J. D. (1998) *Trends Biochem. Sci.* **23,** 454–456.
8. Dangl, J. L. & Jones, J. D. (2001) *Nature* **411,** 826–833.
9. Marathe, R. & Dinesh-Kumar, S. P. (2003) *Mol. Cell* **11,** 284–286.
10. Mackey, D., Holt, B. F., Wiig, A. & Dangl, J. L. (2002) *Cell* **108,** 743–754.
11. Mackey, D., Belkhadir, Y., Alonso, J. M., Ecker, J. R. & Dangl, J. L. (2003) *Cell* **112,** 379–389.
12. Axtell, M. J. & Staskawicz, B. J. (2003) *Cell* **112,** 369–377.
13. Belkhadir, Y., Nimchuk, Z., Hubert, D. A., Mackey, D. & Dangl, J. L. (2004) *Plant Cell* **16,** 2822–2835.
14. Shao, F., Golstein, C., Ade, J., Stoutemyer, M., Dixon, J. E. & Innes, R. W. (2003) *Science* **301,** 1230–1233.
15. Axtell, M. J., Chisholm, S. T., Dahlbeck, D. & Staskawicz, B. J. (2003) *Mol. Microbiol.* **49,** 1537–1546.
16. Jin, P., Wood, M. D., Wu, Y., Xie, Z. & Katagiri, F. (2003) *Plant Physiol.* **133,** 1072–1082.
17. Hellens, R. P., Edwards, E. A., Leyland, N. R., Bean, S. & Mullineaux, P. M. (2000) *Plant Mol. Biol.* **42,** 819–832.
18. Tai, T. H., Dahlbeck, D., Clark, E. T., Gajiwala, P., Pasion, R., Whalen, M. C., Stall, R. E. & Staskawicz, B. J. (1999) *Proc. Natl. Acad. Sci. USA* **96,** 14153–14158.
19. Yamada, K., Lim, J., Dale, J. M., Chen, H., Shinn, P., Palm, C. J., Southwick, A. M., Wu, H. C., Kim, C., Ngyuen, M., *et al.* (2003) *Science* **302,** 842–846.
20. Turner, P., Barber, C. & Daniels, M. (1984) *Mol. Gen. Genet.* **195,** 101–107.
21. Figurski, D. H. & Helinski, D. R. (1979) *Proc. Natl. Acad. Sci. USA* **76,** 1648–1652.
22. Harlow, E. & Lane, D. (1999) *Using Antibodies: A Laboratory Manual* (Cold Spring Harbor Lab. Press, Plainview, NY).
23. Mudgett, M. B. & Staskawicz, B. J. (1999) *Mol. Microbiol.* **32,** 927–941.
24. Bailey, T. L. & Elkan, C. (1994) in *Proceedings of the Second International Conference on Intelligent Systems for Molecular Biology* (AAAI Press, Menlo Park, CA), pp. 28–36.
25. Jones, D. A. & Takemoto, D. (2004) *Curr. Opin. Immunol.* **16,** 48–62.
26. Lim, M. T. & Kunkel, B. N. (2004) *Plant J.* **40,** 790–798.
27. Hotson, A., Chosed, R., Shu, H., Orth, K. & Mudgett, M. B. (2003) *Mol. Microbiol.* **50,** 377–389.
28. Roden, J., Eardley, L., Hotson, A., Cao, Y. & Mudgett, M. B. (2004) *Mol. Plant–Microbe Interact.* **17,** 633–643.